JCI The Journal of Clinical Investigation

β2 adrenergic receptor–mediated signaling regulates the immunosuppressive potential of myeloid-derived suppressor cells

Hemn Mohammadpour, … , Scott I. Abrams, Elizabeth A. Repasky

J Clin Invest. 2019;129(12):5537-5552. https://doi.org/10.1172/JCI129502.

Research Article **Immunology** **Oncology**

Catecholamines released by sympathetic nerves can activate adrenergic receptors present on nearly every cell type, including myeloid-derived suppressor cells (MDSCs). Using in vitro systems, murine tumor models in wild-type and genetically modified (β2-AR$^{-/-}$) mice, and adoptive transfer approaches, we found that the degree of β2-AR signaling significantly influences MDSC frequency and survival in tumors and other tissues. It also modulates their expression of immunosuppressive molecules such as arginase-I and PD-L1 and alters their ability to suppress the proliferation of T cells. The regulatory functions of β2-AR signaling in MDSCs were also found to be dependent upon STAT3 phosphorylation. Moreover, we observed that the β2-AR–mediated increase in MDSC survival is dependent upon Fas-FasL interactions, and this is consistent with gene expression analyses, which reveal a greater expression of apoptosis-related genes in β2-AR$^{-/-}$ MDSCs. Our data reveal the potential of β2-AR signaling to increase the generation of MDSCs from both murine and human peripheral blood cells and that the immunosuppressive function of MDSCs can be mitigated by treatment with β-AR antagonists, or enhanced by β-AR agonists. This strongly supports the possibility that reducing stress-induced activation of β2-ARs could help to overcome immune suppression and enhance the efficacy of immunotherapy and other cancer therapies.

β2 adrenergic receptor–mediated signaling regulates the immunosuppressive potential of myeloid-derived suppressor cells

Hemn Mohammadpour,[1] Cameron R. MacDonald,[1] Guanxi Qiao,[1] Minhui Chen,[1] Bowen Dong,[1] Bonnie L. Hylander,[1] Philip L. McCarthy,[2] Scott I. Abrams,[1] and Elizabeth A. Repasky[1]

[1]Department of Immunology, and [2]Department of Medicine, Roswell Park Comprehensive Cancer Center, Buffalo, New York, USA.

Catecholamines released by sympathetic nerves can activate adrenergic receptors present on nearly every cell type, including myeloid-derived suppressor cells (MDSCs). Using in vitro systems, murine tumor models in wild-type and genetically modified (β2-AR$^{-/-}$) mice, and adoptive transfer approaches, we found that the degree of β2-AR signaling significantly influences MDSC frequency and survival in tumors and other tissues. It also modulates their expression of immunosuppressive molecules such as arginase-I and PD-L1 and alters their ability to suppress the proliferation of T cells. The regulatory functions of β2-AR signaling in MDSCs were also found to be dependent upon STAT3 phosphorylation. Moreover, we observed that the β2-AR–mediated increase in MDSC survival is dependent upon Fas-FasL interactions, and this is consistent with gene expression analyses, which reveal a greater expression of apoptosis-related genes in β2-AR$^{-/-}$ MDSCs. Our data reveal the potential of β2-AR signaling to increase the generation of MDSCs from both murine and human peripheral blood cells and that the immunosuppressive function of MDSCs can be mitigated by treatment with β-AR antagonists, or enhanced by β-AR agonists. This strongly supports the possibility that reducing stress-induced activation of β2-ARs could help to overcome immune suppression and enhance the efficacy of immunotherapy and other cancer therapies.

Introduction

A major hallmark of cancer cells is their ability to avoid immune detection and destruction. One mechanism of tumor immune escape is through the accumulation of several immune cell populations, including myeloid-derived suppressor cells (MDSCs), tumor-associated macrophages (TAMs), and regulatory T cells (Tregs), which exhibit potent immune suppressive activities (1–4). MDSCs are immature myeloid cells that share some characteristics with monocytes and neutrophils but have distinct functional differences. These include their ability to release soluble immunosuppressive factors and promote angiogenesis and metastasis (1, 5). There are 2 distinct subsets of MDSCs: monocytic MDSCs (M-MDSCs; CDllb^{+}Ly6G^{-}Ly6C^{hi}) and granulocytic or polymorphonuclear (PMN) MDSCs (PMN-MDSCs; CDllb^{+}Ly6G^{+}Ly6C^{lo}), which differ somewhat in their ability to suppress immune responses (6–9). Although the protumor, immunosuppressive potential of MDSCs is well-recognized, the mechanisms through which they acquire their inhibitory functions, especially under physiological conditions, remain incompletely understood.

Several studies in mice and humans reinforce the growing recognition of a negative role for various forms of chronic stress and their activation of the sympathetic nervous system (SNS) stress response in cancer progression, metastasis, and drug resistance (10–15). Nerve fibers present in and around most tissues and organs, as well as tumors (13, 16, 17), release neurotransmitters and other neuropeptides locally and systemically. The release of catecholamines (norepinephrine [NE] and epinephrine) by ubiquitously distributed sympathetic nerves, and by some special cells such as tyrosine hydroxylase–positive cells in the spleen, can directly stimulate cells bearing adrenergic receptors (ARs) (18). ARs belong to the guanine nucleotide–binding G protein–coupled receptor (GPCR) superfamily (19). Two classes of ARs have been identified: α-ARs and β-ARs. The α1-AR is primarily expressed on endothelial cells of blood vessels, whereas the α2-AR is more ubiquitously expressed. β-ARs comprise 3 receptors, including β1, β2, and β3. β1 and β3 receptors are primarily expressed in heart and adipose tissues respectively, whereas β2-AR is expressed by most cells, including immune cells (20–22).

Many effects of adrenergic signaling in immune cells have been reported in previous studies. For example, β2-AR activation in T cells was seen to suppress their ability to secrete interferon-γ (IFN-γ) in response to infection with vesicular stomatitis virus (23) and impair metabolic reprogramming during T cell activation (11). High levels of NE also impair dendritic cell (DC) maturation (24, 25) and increase MDSC recruitment into the tumor microenvironment (TME) (26). Murine studies from our lab showed that chronic β2-AR signaling suppresses antitumor CD8^{+} T cell function and increases populations of MDSCs and Tregs in the spleen and tumor microenvironment, respectively (27, 28). However, the role of β2-AR in major aspects of MDSC functions associated with suppressing the

▶ Related Commentary: p. 5086

Conflict of interest: The authors have declared that no conflict of interest exists.

Submitted: April 19, 2019; **Accepted:** September 18, 2019; **Published:** November 11, 2019.
Reference information: *J Clin Invest*. 2019;129(12):5537–5552.
https://doi.org/10.1172/JCI129502.

antitumor immune response, including their generation and accumulation, immune-regulatory function, and survival, have not been addressed. The fact that stress-induced catecholamines are rapidly released systemically, indicates the potential for physiological mechanisms to influence the overall balance of immune factors dictating tumor progression and highlights a critical need to understand how MDSCs are regulated by neural activity.

Here we tested whether β2-AR signaling plays a major role in dictating the immunosuppressive function of MDSCs in the TME and in other tissues including the spleen and blood. Using in vitro and in vivo strategies, including use of β2-AR–deficient mice (referred to as β2-AR$^{-/-}$) and adoptive transfer models, we examined the impact of adrenergic stress signaling through β2-ARs on MDSC frequency in tumors and other tissues, whether the β2-AR expression in MDSCs is influenced by expression of cytokines including GM-CSF, and how β2-AR signaling modulates the expression of immunosuppressive molecules such as arginase-I and PD-L1 in MDSCs. We also examined the impact of β2-AR signaling on the immune regulatory functions of MDSCs on T cells, the survival of MDSCs in tumor and peripheral tissues, and the generation of MDSCs from human and mouse models cells. Our data reveal a major impact of β2-AR signaling on the immune suppressive potential of MDSCs and suggest that reducing stress-induced activation of β2-AR could help to overcome immune suppression and enhance the efficacy of immunotherapy and other cancer therapies.

Results

Chronic stress–mediated β2 adrenergic signaling increases MDSC dependent tumor growth. Our laboratory has relied on several in vivo models (28, 29) to investigate the effects of adrenergic stress on cancer progression. Here, we sought to determine whether the immune suppressive activity of MDSCs plays a key role in driving the increased tumor growth rates we have observed in these and other models. To this end, we first set up several models to obtain material for the analyses shown in subsequent data. We used a physiological model of adrenergic stress (29) in which NE levels can be manipulated by housing mice at either the standard subthermoneutral housing temperature (ST; ~22°C), or a thermoneutral housing temperature (TT; ~30°C). When housed at ST, the sympathetic nervous system is activated, and NE production is increased to drive thermogenesis (30). Conversely, thermogenesis is not needed at TT, adrenergic stress is reduced, and NE levels are decreased (12, 28). As observed in our earlier studies, (27) we found that mice housed under TT conditions showed delayed tumor growth (Figure 1, A and B) and decreased tumor weights (Supplemental Figure 2A; supplemental material available online with this article; https://doi.org/10.1172/JCI129502DS1). Here, we also report that at TT conditions there are reduced levels of circulating protumor cytokines (Supplemental Figure 1, A and B) compared with mice housed at ST conditions. As the β2-AR is the most prominent AR expressed by immune cells (31), we compared tumor growth in BALB/c WT mice and β2-AR$^{-/-}$ mice. As we previously observed (28), 4T1 tumors grew at a decreased rate in β2-AR$^{-/-}$ mice (Figure 1C and Supplemental Figure 2B). Here, we also found decreased levels of several protumor cytokines in the plasma (Supplemental Figure 1C) and, together with the data in Supplemental Figure 1, A and B, these results suggest a role for the β2-AR pathway in regulating the overall cytokine milieu in tumor-bearing mice. Consistent with these data, we found that the lungs of β2-AR$^{-/-}$ mice had fewer metastatic nodules (Supplemental Figure 2C).

We next made bone marrow chimeras, using the BALB/c WT and β2-AR$^{-/-}$ models defined below, to test whether the impact of β2-AR signaling on tumor growth was dependent upon cells of hematological origin or stromal cells of the tumor. Lethally irradiated BALB/c WT mice and β2-AR$^{-/-}$ mice were reconstituted with BM cells isolated from either β2-AR$^{-/-}$ mice or WT controls. We found that the growth of 4T1 tumors was significantly slower in mice reconstituted with β2-AR$^{-/-}$ BM than in mice reconstituted with WT BM (Figure 1D), suggesting that β2-AR signaling in a cell type derived from the bone marrow plays a key role in tumor growth promotion.

In investigating which specific type(s) of hematopoietic cells are most important in this process, we focused on MDSCs, as they are a relevant population of hematopoietic cells known to be associated with immune suppression and cancer progression. To test whether β2-AR$^{-/-}$ deficient MDSCs lose their protumorigenic properties, we depleted MDSCs in both WT and β2-AR$^{-/-}$ mice using an anti–Gr-1 antibody (31). MDSC depletion significantly delayed 4T1 tumor growth in WT mice, but led only to a small, nonsignificant decrease tumor growth rate in β2-AR$^{-/-}$ mice (Figure 1E). These data confirm that MDSCs from WT mice promote tumor growth, while tumor growth in β2-AR$^{-/-}$ mice is not affected by β2-AR$^{-/-}$ MDSCs.

So far, we have demonstrated that the impact of adrenergic stress on tumor growth is largely dependent on MDSCs, but the precise role adrenergic signaling in MDSCs plays in altering tumor growth rates has not yet been determined. To this end, we first visualized the expression of β2-ARs on MDSCs from 4T1 tumor-bearing WT and β2-AR$^{-/-}$ mice via ImageStream. After confirming β2-AR expression in WT but not β2-AR$^{-/-}$ MDSCs (Figure 1F), we sought to further determine whether the presence of a tumor altered the level of β2-AR expression in WT MDSCs. When comparing MDSCs from the spleens of tumor-bearing mice to those that were isolated from the spleens of healthy mice, we observed a significant increase in β2-AR expression in MDSCs from the spleens of tumor-bearing mice (Figure 1I).

When considering this variability in β2-AR expression in conjunction with the observed changes in cytokine levels in earlier experiments (Supplemental Figure 1, A–C), we sought to investigate whether increased cytokine levels originating from the TME might be involved in locally increasing the expression of β2-AR in intratumoral MDSCs. To address this question, we cultured MDSCs sorted from the BM of non–tumor bearing mice with either IL-6, granulocyte-macrophage colony-stimulating factor (GM-CSF), or lipopolysaccharide (LPS) as a standard activator of MDSCs. We found that GM-CSF and LPS treatments were associated with an increase in β2-AR expression, whereas treatment with IL-6 was not (Figure 1, G and H), suggesting that β2-AR expression in MDSCs is differentially responsive to various cytokines. The ability of GM-CSF, which is found at high levels in the plasma of tumor-bearing mice (32), to induce expression of β2-ARs in MDSCs correlates with our finding that a higher percentage of the splenic MDSCs from tumor-bearing mice express β2-ARs compared with those from non–tumor bearing mice (Figure 1I). Altogether,

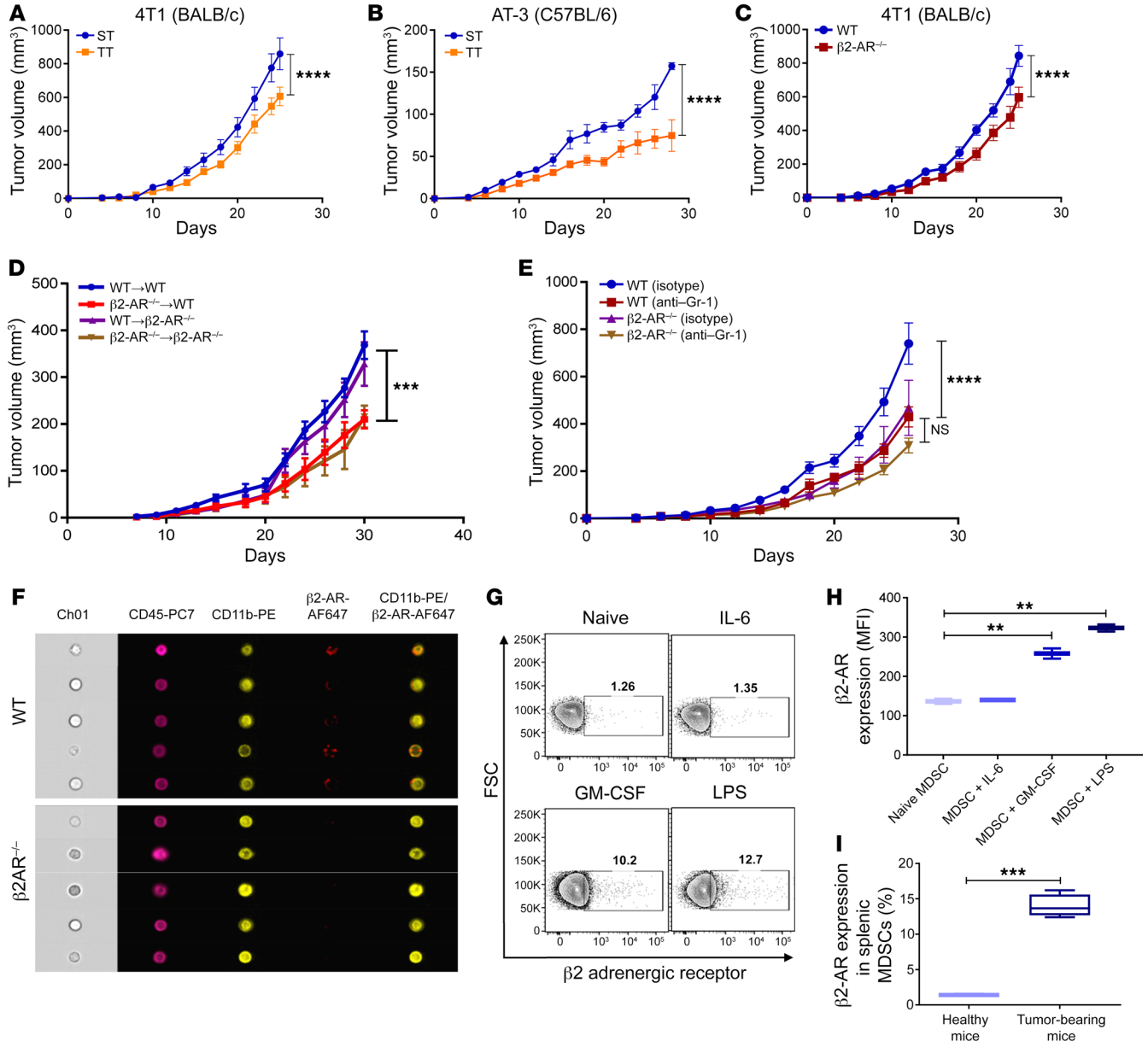

Figure 1. β2-AR activation increases tumor growth in a MDSC-dependent manner. (**A** and **B**) Tumor growth in mice bearing 4T1 and AT-3 tumor cells, housed at ST (22°C) or TT (30°C). (**C**) Tumor growth kinetics in WT and β2-AR$^{-/-}$ mice bearing 4T1 tumor cells. (**D**) Lethally irradiated WT mice received bone marrow transplants from WT (blue circle) or β2-AR$^{-/-}$ (red square) mice. Lethally irradiated β2-AR$^{-/-}$ mice received bone marrow transplants from WT (purple triangle) or β2-AR$^{-/-}$ (brown triangle) mice. Eight weeks after transplantation, chimeric mice were injected with 4T1 tumor cells and tumor growth was monitored. (**E**) 4T1 tumor–bearing WT or β2-AR$^{-/-}$ mice were injected with isotype or anti–Gr-1 antibodies (200 μg per mouse, i.p., every 4 days), and tumor growth was monitored. (**F**) β2-AR expression in MDSCs sorted by MDSC isolation kit from spleen of 4T1 tumor–bearing mice 25 days after tumor injection using Image Stream. (**G** and **H**) β2-AR expression in MDSCs sorted from bone marrow of non–tumor bearing mice after culture with IL-6, G-CSF, and LPS (data from 3 independent replicates). (**I**) The levels of β2-AR in splenic MDSCs from healthy or 4T1 tumor–bearing mice using flow cytometry. Two-way ANOVA was used to analyze statistical significance among tumor growth in different groups. These data are presented as mean ± SEM of 5 mice per group from at least 2 replicate experiments. Other data are presented as median ± minimum to maximum. One-way ANOVA was used to analyze statistical significance among 4 groups, and the Student's *t* test was used to analyze statistical significance between 2 groups. In all panels, $^{**}P < 0.01$, $^{***}P < 0.001$ and $^{****}P < 0.0001$. A *P* value less than 0.05 was considered significant.

these data demonstrate that there is a tight association between tumor-promoting cytokines, β2-AR expression on MDSCs, and MDSC-dependent tumor growth such that the whole response may be orchestrated by sympathetic nervous system activity.

β2-AR activation during chronic stress increases MDSC accumulation and tumor vascularization. We next tested the role of β2-AR in MDSC accumulation in the spleen, TME, and other tissues. 4T1 cells were injected into WT or β2-AR$^{-/-}$ mice and on day 25, MDSC accumulation in blood, lymph node, lung, spleen, and tumor was quantified by flow cytometry. We found that the percentage of CD11b^{+} myeloid cells within the live CD45^{+} cells of the TME was significantly elevated in WT mice compared with β2-AR$^{-/-}$ mice

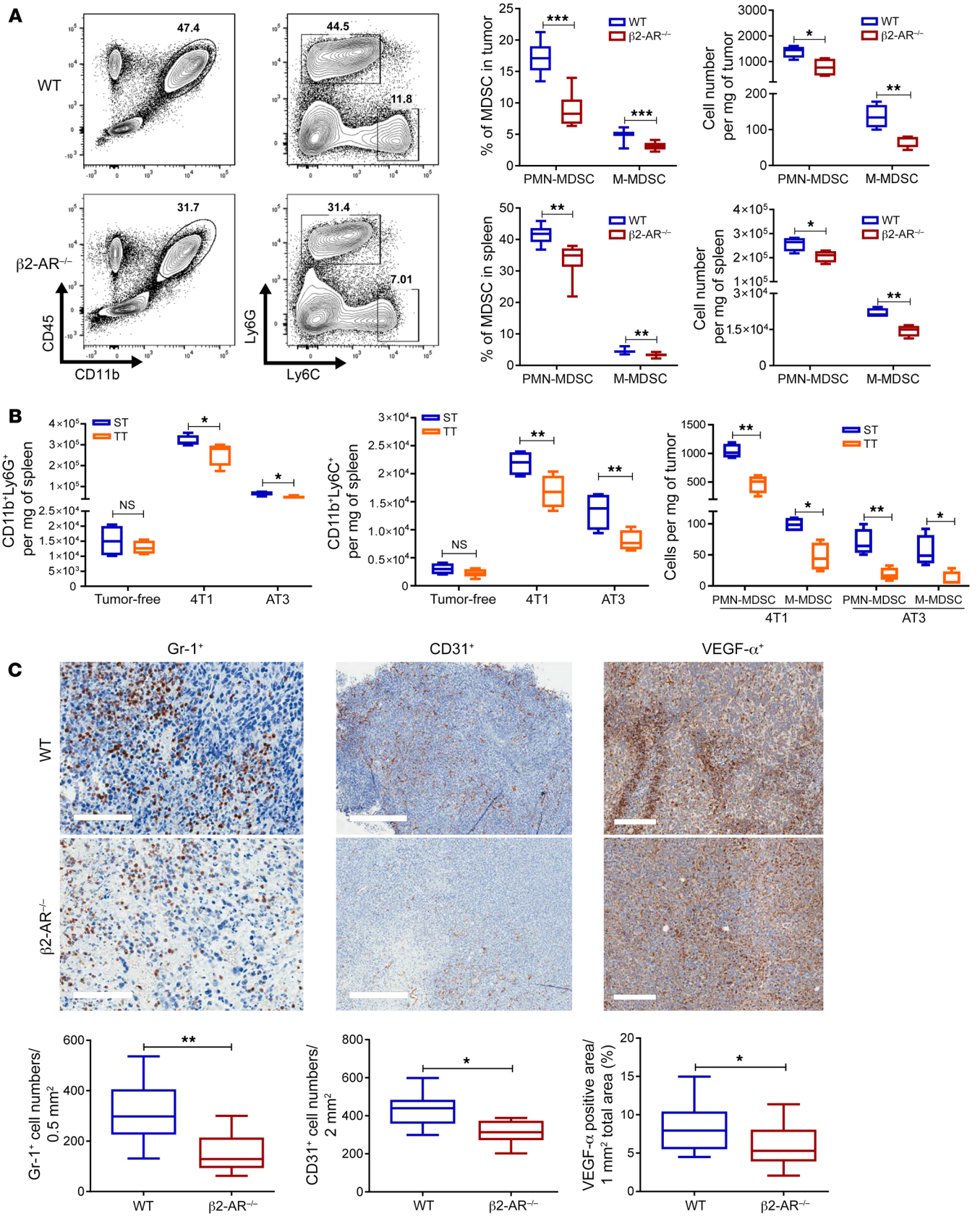
A
WT
β2-AR−/−
47.4
44.5
11.8
31.7
31.4
7.01
CD45
CD11b
Ly6G
Ly6C
% of MDSC in tumor
% of MDSC in spleen
Cell number per mg of tumor
Cell number per mg of spleen
PMN-MDSC
M-MDSC
WT
β2-AR−/−
B
CD11b+Ly6G+ per mg of spleen
CD11b+Ly6C+ per mg of spleen
Cells per mg of tumor
ST
TT
NS
Tumor-free
4T1
AT3
C
Gr-1+
CD31+
VEGF-α+
Gr-1+ cell numbers/ 0.5 mm2
CD31+ cell numbers/ 2 mm2
VEGF-α positive area/ 1 mm2 total area (%)

Figure 2. β2-AR activation during chronic stress increases MDSC accumulation in the spleen and tumor. (**A**) Representative flow cytometry analysis of PMN-MDSC and M-MDSC subpopulations, as well as absolute number of PMN-MDSCs and M-MDSCs in tumor and spleen of 4T1 tumor–bearing mice on day 25 after tumor injection. The data presented are from groups of 10 mice from 2 replicate studies. (**B**) Absolute number of G-MDSCs and M-MDSCs in tumor and spleen of healthy or tumor-bearing mice (4T1 or AT-3) at day 25 after tumor injection housed in ST or TT. The data presented are from groups of 8 mice from 2 replicate studies. (**C**) Both representative immunohistochemistry analysis and absolute number of Gr-1– (×20 magnification, scale bars = 100 μm), CD31- (×4 magnification, scale bars: 500 μm) and VEGF-α–positive (×10 magnification, scale bars: 200 μm) cells in 4T1 tumors at day 25 after tumor injection. These data are presented as median ± minimum to maximum from groups of 6 mice from 2 replicate studies. The Student's *t* test was used to analyze statistical significance between 2 groups. In all panels, $*P < 0.05$, $**P < 0.01$, and $***P < 0.001$. A *P* value less than 0.05 was considered significant.

(Figure 2A). In β2-AR$^{-/-}$ mice, we observed significantly fewer PMN-MDSCs and M-MDSCs, suggesting that the expression of β2-ARs on MDSCs increases the accumulation of both subsets in tumor-bearing mice. The absolute number of MDSCs was also higher in both the spleen and tumor tissue of WT mice compared with β2-AR$^{-/-}$ mice (Figure 2A). In addition, we found that housing mice under TT conditions significantly decreased MDSC accumulation in the spleen and TME in both tumor models, but we found no significant differences in phenotypically similar populations in tumor-free mice (Figure 2B). We also found that the accumulation of MDSCs significantly increased in both blood and lymph node tissues of 4T1 tumor-bearing mice housed at ST compared with TT (Supplemental Figure 3, A and B). We also assessed the accumulation of MDSCs in lung tissue of WT and β2-AR$^{-/-}$ mice bearing either 4T1 tumors, which are metastatic, or AT-3 tumors, which are nonmetastatic. We found that the lungs of β2-AR$^{-/-}$ mice had significantly fewer numbers of MDSCs compared with WT mice in the 4T1 tumor model, but this was not observed in the AT-3 tumor model (Supplemental Figure 3C). Thus, our results show that tumor growth and metastasis is diminished in mice that lack β2-ARs. To extend our flow cytometry findings, we performed immunohistochemistry to analyze myeloid cell accumulation, labeled by Gr-1, and angiogenesis, labeled by CD31 and VEGF-α in the TME. We observed an increase in the proportion of Gr-1$^+$ and CD31$^+$ cells in WT mice compared with β2-AR$^{-/-}$ mice (Figure 2C). We also found that the VEGF-α–positive area was significantly higher in WT mice compared with β2-AR$^{-/-}$ mice (Figure 2C). Taken together, these data suggest that chronic stress, signaling through β2-AR, increases the accumulation of myeloid cells which in turn could be enhancing tumor growth by vascularization through β2-AR–dependent signaling and/or other mechanisms.

β2-AR activation increases the immune-inhibitory activity of MDSCs. So far, we have demonstrated that chronic stress–mediated β2-AR activation increases the accumulation of MDSCs in tumors, enhances tumor vascularization, and augments the level of tumor-promoting cytokines in the plasma of tumor-bearing mice. We have also shown that protumor effects of β2-AR are associated with the expression of β2-AR on hematopoietic cells rather than stromal cells. We next tested the impact of β2-AR activation on the function of MDSCs in vitro. To this end, we isolated total BM cells and generated MDSCs using a GM-CSF and IL-6 cytokine cocktail, as described (33). The addition of the β-AR agonist isoproterenol (ISO) to the culture significantly increased the expression of well-known immunosuppressive molecules, such as arginase I and programmed death ligand 1 (PD-L1), in MDSCs compared with the control group, and this increase was inhibited by the addition of propranolol (a β-AR blocker; Figure 3A). To test the functional activity of ISO-treated MDSCs, we performed a T cell proliferation assay. After coculture of WT control MDSCs or ISO-treated MDSCs, we observed that ISO-treated MDSCs were significantly more immunosuppressive against both CD8$^+$ and CD4$^+$ T cell proliferation (Figure 3B) compared with the controls. Furthermore, we used flow cytometry to assess levels of arginase I and PD-L1 in MDSCs isolated from 4T1 tumors, and found that intratumoral WT MDSCs have a significantly higher level of arginase I and PD-L1 compared with β2-AR$^{-/-}$ MDSCs (Supplemental Figure 4A). Then, we sorted WT and β2-AR$^{-/-}$ MDSCs from tumor tissue and cocultured them with CD4$^+$ and CD8$^+$ T cells. Inhibition of T cell proliferation was significantly greater with WT MDSCs compared with β2-AR$^{-/-}$ MDSCs (Supplemental Figure 4B). These data demonstrate that β2-AR signaling in MDSCs increases the immunosuppressive function of MDSCs.

In line with this reduced immunosuppressive ability, we hypothesized that β2-AR$^{-/-}$ MDSCs would have a less immunosuppressive phenotype. Therefore, we compared immune-related gene expression patterns of WT and β2-AR$^{-/-}$ MDSCs by comparing sorted WT and β2-AR$^{-/-}$ MDSCs from tumors by Nanostring analysis. Nanostring data showed that WT MDSCs expressed higher levels of the immunosuppressive molecules (*Il11ra*, *Ahr*, *Cd209*, *Dpp4*, *Xcr1*, *Gpr44*) and cytokines (*Il4*, *Il2*, *Il5*, *Il33*, *Il-21*) than did β2-AR$^{-/-}$ MDSCs (Figure 3C). Conversely, the expression of the costimulatory markers (*Cd86*, *Cd40*, *Cd83*, *Cd27*, *Cd6*, and *Tlr8*) and antitumor cytokines (*Ifng*, *Il12a*, *Il12b*) was higher in β2-AR$^{-/-}$ MDSCs (Figure 3C). Furthermore, to confirm the different phenotypes, MDSCs were isolated from the BM of WT or β2-AR$^{-/-}$ 4T1 tumor–bearing mice, activated with LPS for 18 hours, and the levels of protumor and antitumor cytokines were measured. Significant increases in protumor cytokine production were observed in WT MDSCs, compared with β2-AR$^{-/-}$ MDSCs. Conversely, we observed that the secretion of IFN-γ by β2-AR$^{-/-}$ MDSCs was significantly increased compared with WT MDSCs (Figure 3D).

To examine the importance of β2-AR expression for MDSC protumorigenic function in vivo, 4T1 cells were mixed 1:1 with MDSCs isolated from WT or β2-AR$^{-/-}$ 4T1 tumor–bearing mice, and injected orthotopically into fresh groups of WT mice. Coinjection of 4T1 with β2-AR$^{-/-}$ MDSCs into WT mice resulted in significantly delayed tumor growth compared with coinjection with WT MDSCs (Figure 3E), suggesting that the expression of β2-AR on MDSCs plays an important role in inducing MDSC-mediated protumor mechanisms. We next evaluated the immunosuppressive capabilities of WT or β2-AR$^{-/-}$ MDSCs by an adoptive transfer approach. The adoptive transfer of WT MDSCs into β2-AR$^{-/-}$ mice increased tumor growth, whereas the adoptive transfer of β2-AR$^{-/-}$ MDSCs 3 or 6 days after 4T1 implantation delayed tumor growth (Figure 3F). These data show that β2-AR expression and activation in MDSCs are necessary for the immunosuppressive function of MDSCs and promotion of tumor growth.

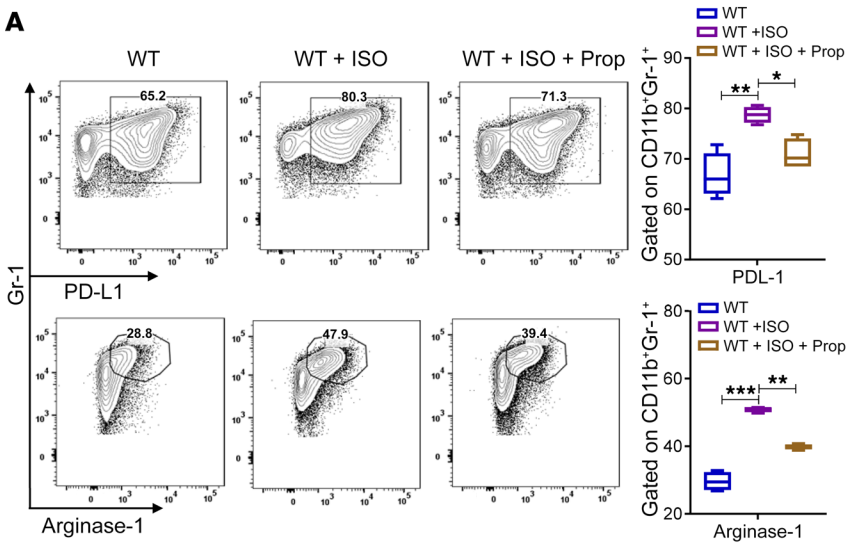
A
WT
WT + ISO
WT + ISO + Prop
65.2
80.3
71.3
Gr-1
PD-L1
28.8
47.9
39.4
Arginase-1
WT
WT +ISO
WT + ISO + Prop
Gated on CD11b+Gr-1+
PDL-1
Arginase-1

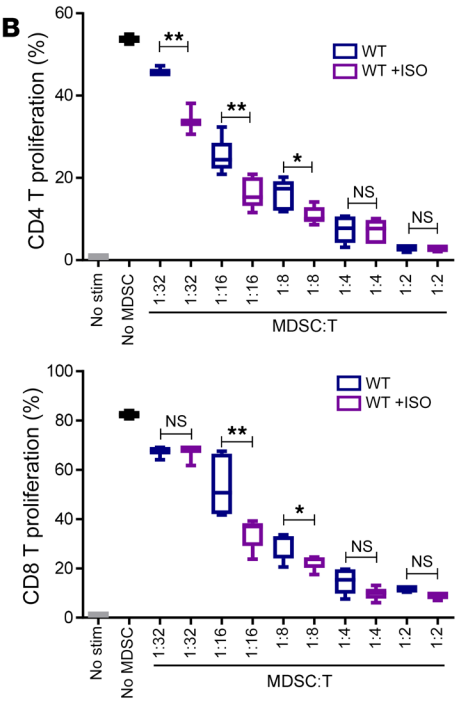
B
CD4 T proliferation (%)
CD8 T proliferation (%)
WT
WT +ISO
No stim
No MDSC
1:32
1:16
1:8
1:4
1:2
MDSC:T

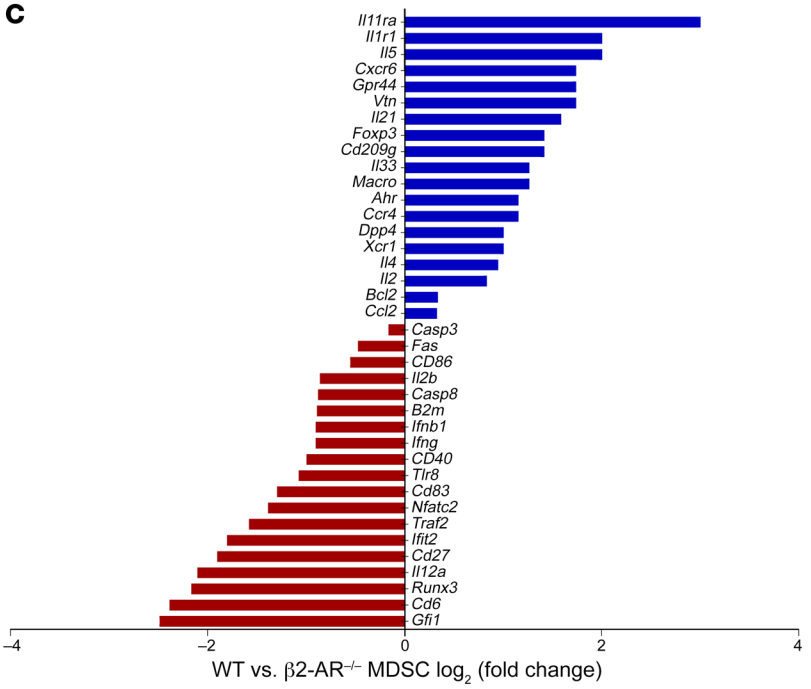
C
Il11ra
Il1r1
Il5
Cxcr6
Gpr44
Vtn
Il21
Foxp3
Cd209g
Il33
Macro
Ahr
Ccr4
Dpp4
Xcr1
Il4
Il2
Bcl2
Ccl2
Casp3
Fas
CD86
Il2b
Casp8
B2m
Ifnb1
Ifng
CD40
Tlr8
Cd83
Nfatc2
Traf2
Ifit2
Cd27
Il12a
Runx3
Cd6
Gfi1
WT vs. β2-AR−/− MDSC log2 (fold change)

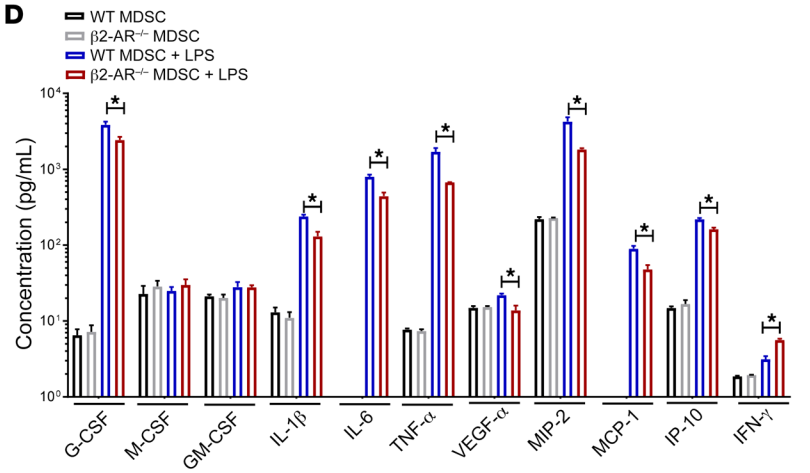
D
WT MDSC
β2-AR−/− MDSC
WT MDSC + LPS
β2-AR−/− MDSC + LPS
Concentration (pg/mL)
G-CSF
M-CSF
GM-CSF
IL-1β
IL-6
TNF-α
VEGF-α
MIP-2
MCP-1
IP-10
IFN-γ

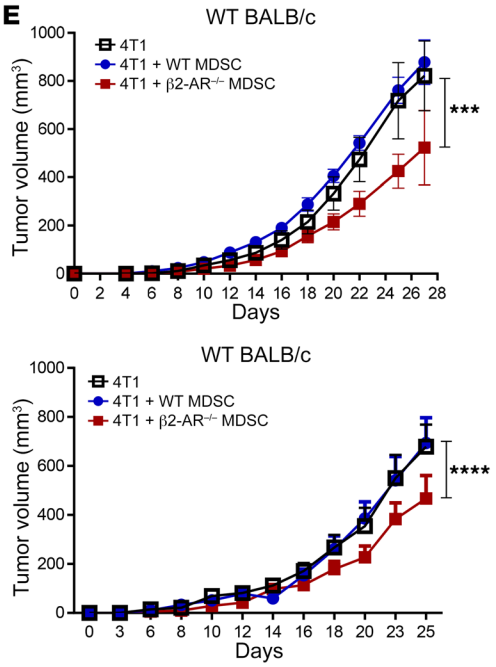
E
WT BALB/c
4T1
4T1 + WT MDSC
4T1 + β2-AR−/− MDSC
Tumor volume (mm3)
Days
WT BALB/c
4T1
4T1 + WT MDSC
4T1 + β2-AR−/− MDSC
Tumor volume (mm3)
Days

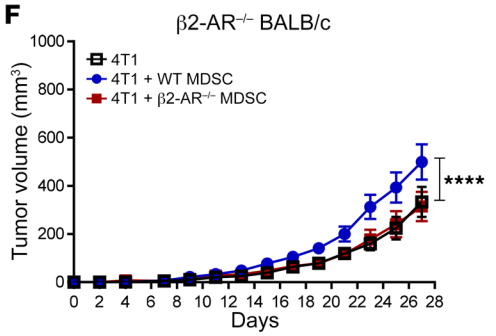
F
β2-AR−/− BALB/c
4T1
4T1 + WT MDSC
4T1 + β2-AR−/− MDSC
Tumor volume (mm3)
Days

Figure 3. β2-AR deletion decreases the immune suppressive activity of MDSCs. (**A**) Representative flow cytometry data of the expression of arginase I and PDL-1 plus the percentage of arginase I and PD-L1 in MDSCs derived from bone marrow in the presence of IL-6 and GM-CSF (WT), IL-6, GM-CSF and ISO (WT + ISO) or IL-6, GM-CSF, and ISO and Prop (WT + ISO + Prop) for 6 days. (**B**) T cells cocultured with WT or WT + ISO MDSCs in various ratios (n = 3). (**C**) Nanostring nCounter microarray analysis of WT or β2-AR$^{-/-}$ MDSCs sorted by flow cytometry from 4T1 tumors of WT or β2-AR$^{-/-}$ mice 25 days after tumor injection (WT or β2-AR$^{-/-}$ MDSCs were pooled from 5 mice per group). (**D**) WT and β2-AR$^{-/-}$ MDSCs were sorted from bone marrow of 4T1 tumor–bearing mice, cultured with LPS for 24 hours, and cytokines levels were analyzed in culture media using multiplex (n = 3). (**E**) Tumor growth kinetics in WT mice orthotopically injected with 4T1 cells (black square) or coinjected with 4T1 cells and WT MDSCs (blue circle) or 4T1 cells and β2-AR$^{-/-}$ MDSCs (red square). MDSCs were sorted from the BM of tumor-bearing mice using an MDSC isolation kit. (**F**) Tumor growth kinetics in WT or β2-AR$^{-/-}$ mice receiving i.v. transfer (3×10^6 on days 3 and 6 after 4T1 injection) of MDSCs sorted the BM of tumor-bearing WT or β2-AR$^{-/-}$ mice. Two-way ANOVA was used to analyze statistical significance among tumor growth in different groups. These data are presented as mean ± SEM. Other data are presented as median ± minimum to maximum. One-way ANOVA was used to analyze statistical significance among 3 groups, and the Student's t test was used to analyze statistical significance between 2 groups. In all panels, $^*P < 0.05$, $^{**}P < 0.01$, $^{***}P < 0.001$, and $^{****}P < 0.0001$. A P value less than 0.05 was considered significant.

β2-AR expression plays an important role in MDSC turnover and survival. Based on our Nanostring data from WT and β2-AR$^{-/-}$ MDSCs sorted from 4T1 tumor–bearing mice, we next asked whether adrenergic stress signaling affected the expression of survival factors in MDSCs themselves. Expression of proapoptotic genes such as *Fas*, *Casp8*, and *Casp3* was higher in β2-AR$^{-/-}$ MDSCs (Figure 3C), whereas the expression of the antiapoptotic gene *Bcl2* was higher in WT MDSCs (Figure 3C). It has been shown that Fas-FasL interactions play an important role in regulating MDSC populations in different tissues (34). Therefore, we hypothesized that deletion of β2-AR increased susceptibility of MDSCs to apoptosis through Fas-FasL interactions.

We quantified the expression of Fas on WT or β2-AR$^{-/-}$ MDSCs and FasL expression on CD8$^+$ T cells (one of the FasL-expressing cells in the TME) in WT and β2-AR$^{-/-}$ 4T1 tumor–bearing mice. The data showed that β2-AR$^{-/-}$ MDSCs expressed Fas at a significantly higher level than WT MDSCs (Figure 4A). Interestingly, β2-AR$^{-/-}$ CD8$^+$ T cells expressed more FasL compared with WT CD8$^+$ T cells (Figure 4A), implicating a likely source of the cognate ligand for Fas engagement. Additionally, higher levels of FasL on β2-AR$^{-/-}$ CD8$^+$ T cells suggest a higher degree of activation, as FasL is upregulated in response antigenic challenges. Furthermore, we observed that WT MDSCs expressed a significantly higher level of the protein B cell lymphoma 2 (BCL-2) compared with β2-AR$^{-/-}$ MDSCs (Figure 4B), suggesting that WT MDSCs are less sensitive to apoptosis compared with β2-AR$^{-/-}$ MDSCs.

To test whether the differential expression of pro- and antiapoptotic molecules by WT and β2-AR$^{-/-}$ MDSCs can influence the survival of MDSCs in the TME, apoptosis of WT or β2-AR$^{-/-}$ MDSCs in 4T1 tumor–bearing mice was investigated. At day 25 after tumor implantation, the level of apoptosis in WT and β2-AR$^{-/-}$ MDSCs was measured in the tumor and spleen tissues. We found that the frequency of apoptotic cells in β2-AR$^{-/-}$ MDSCs was significantly higher, compared with WT MDSCs (Figure 4C) in both tumor and spleen. We also observed a higher level of apoptosis in MDSCs isolated from tumor-bearing mice housed under TT conditions (reduced NE levels) compared with MDSCs isolated from tumor-bearing mice housed under ST conditions (Figure 4C).

To further investigate the importance of β2-AR in MDSC apoptosis, we took advantage of different congenic strains of mice (CD45.1 vs. CD45.2). AT-3 tumor cells, a mammary carcinoma cell line syngeneic to C57BL/6 mice, were orthotopically injected into WT (CD45.1) or β2-AR$^{-/-}$ (CD45.2) mice. On day 25 after tumor injection, we isolated WT (CD45.1) or β2-AR$^{-/-}$ (CD45.2) MDSCs from the tumor-bearing mice, mixed them 1:1, and injected them into fresh groups of AT-3 tumor–bearing GFP-positive mice (Figure 4D). We found that the percentage of WT MDSCs (GFP$^-$ CD45.1$^+$) in the spleen was significantly higher compared with β2-AR$^{-/-}$ MDSCs (GFP$^-$ CD45.2$^+$) at days 3 and 7 after coinjection, suggesting that WT MDSCs could survive longer compared with β2-AR$^{-/-}$ MDSCs (Figure 4E). These data highlight that β2-AR signaling increases the survival of MDSCs in TME at least partially through the Fas-FasL pathway.

β2-AR stimulation activates STAT3 phosphorylation. STAT3 activation in myeloid cells regulates multiple aspects of MDSC biology, including their immunosuppressive function and expansion (35). We hypothesized that ligands of the β2-AR, such as NE and ISO, can activate STAT3 in MDSCs. To test this, MDSCs were isolated from the bone marrow of WT or β2-AR$^{-/-}$ MDSCs from tumor-bearing mice. We then treated WT or β2-AR$^{-/-}$ MDSCs with ISO for different periods of time. Western blot results indicate that ISO induced STAT3 phosphorylation in WT MDSCs after 20 minutes, but not in β2-AR$^{-/-}$ MDSCs (Figure 5A). Moreover, we investigated the in vivo level of phospho-STAT3 (p-STAT3) in MDSCs of 4T1 tumor–bearing mice. These data show that the level of p-STAT3 was significantly higher in WT MDSCs compared with β2-AR$^{-/-}$ MDSCs in both the tumor tissue and spleen. A similar trend was seen in MDSCs isolated from tumor-bearing mice housed at ST compared with TT (Figure 5B), consistent with the notion that physiological chronic stress increases STAT3 activation in MDSCs. To confirm the role of STAT3 activation in these MDSCs, we inhibited STAT3 phosphorylation in 4T1 tumor–bearing mice using the STAT3 inhibitor JSI-124 (36) (Figure 5C). A significant delay in tumor growth was observed in mice receiving the STAT3 inhibitor compared with mice receiving vehicle control in WT but not β2-AR$^{-/-}$ tumor-bearing mice, again supporting a role for β2-AR in STAT3 phosphorylation. Twenty-five days after tumor injection, tumor tissue and spleen were collected. Inhibition of p-STAT3 significantly decreased the number of MDSCs in both tumor tissue and spleen in WT tumor-bearing mice (Figure 5D). These data indicate that the mechanism by which β2-AR signaling enhances accumulation and/or survival of MDSCs occurs through STAT3 phosphorylation, which may lead to increased expression of prosurvival and immunosuppressive genes such as Bcl-2 and arginase-I, respectively, in MDSCs.

β2-AR blockade slows tumor growth and diminishes frequency of MDSCs whereas β-AR agonists accelerate tumor growth and enhance MDSC frequency in the TME. To address the question of whether β2-AR blockade, which slows tumor growth, also reduces MDSC accumulation in the TME, we investigated the effects of proprano-

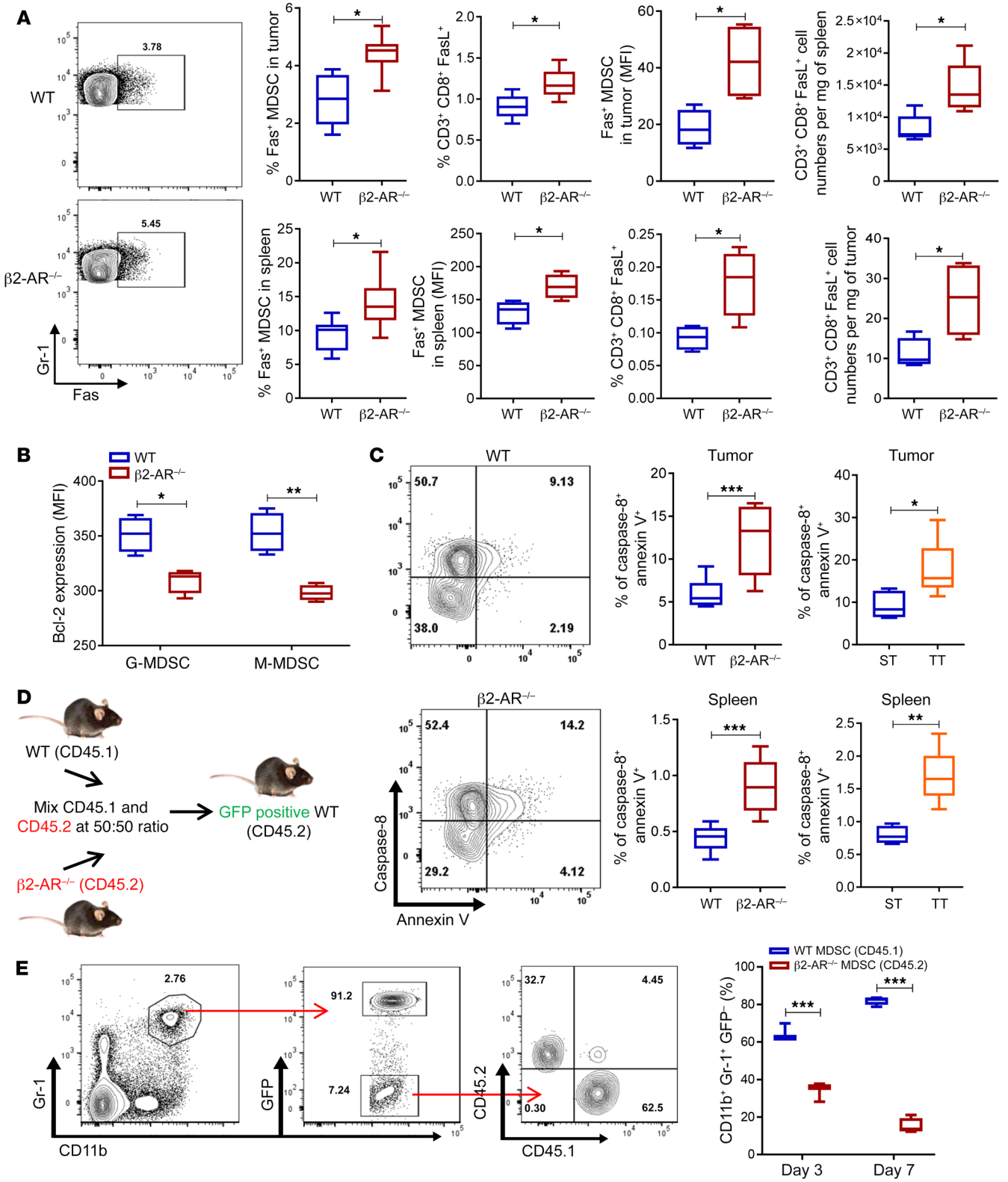

Figure 4. β2-AR prolongs MDSC survival. (**A**) Fas and FasL expression by MDSCs and T cells from WT or β2-AR$^{-/-}$ mice from tumor and spleen, respectively (n = 5). (**B**) Expression of Bcl-2 in intratumoral MDSCs from WT or β2-AR$^{-/-}$ 4T1 tumor–bearing mice (n = 5). (**C**) Levels of apoptosis in MDSCs from tumor and spleen of WT or β2-AR$^{-/-}$ tumor–bearing mice or WT tumor–bearing mice housed at ST or TT. (**D**) Schematic diagram of experimental design to compare the survival capability of WT or β2-AR$^{-/-}$ MDSCs. (**E**) WT (CD45.1) or β2-AR$^{-/-}$ (CD45.2) MDSCs were sorted from bone marrow of AT-3 tumor–bearing mice, mixed in 1:1 ratio, and injected into GFP-positive AT-3 tumor–bearing mice. The percentage of WT (CD45.1) or β2-AR$^{-/-}$ (CD45.2) MDSCs in the live, GFP-negative, CD11b^{+}, and Gr-1^{+} population on day 3 and day 7 after coinjection were analyzed (4 mice per end point). Data are presented as median ± minimum to maximum. The Student's t test was used to analyze statistical significance between 2 groups. In all panels, *P < 0.05, **P < 0.01, and ***P < 0.001. A P value less than 0.05 was considered significant.

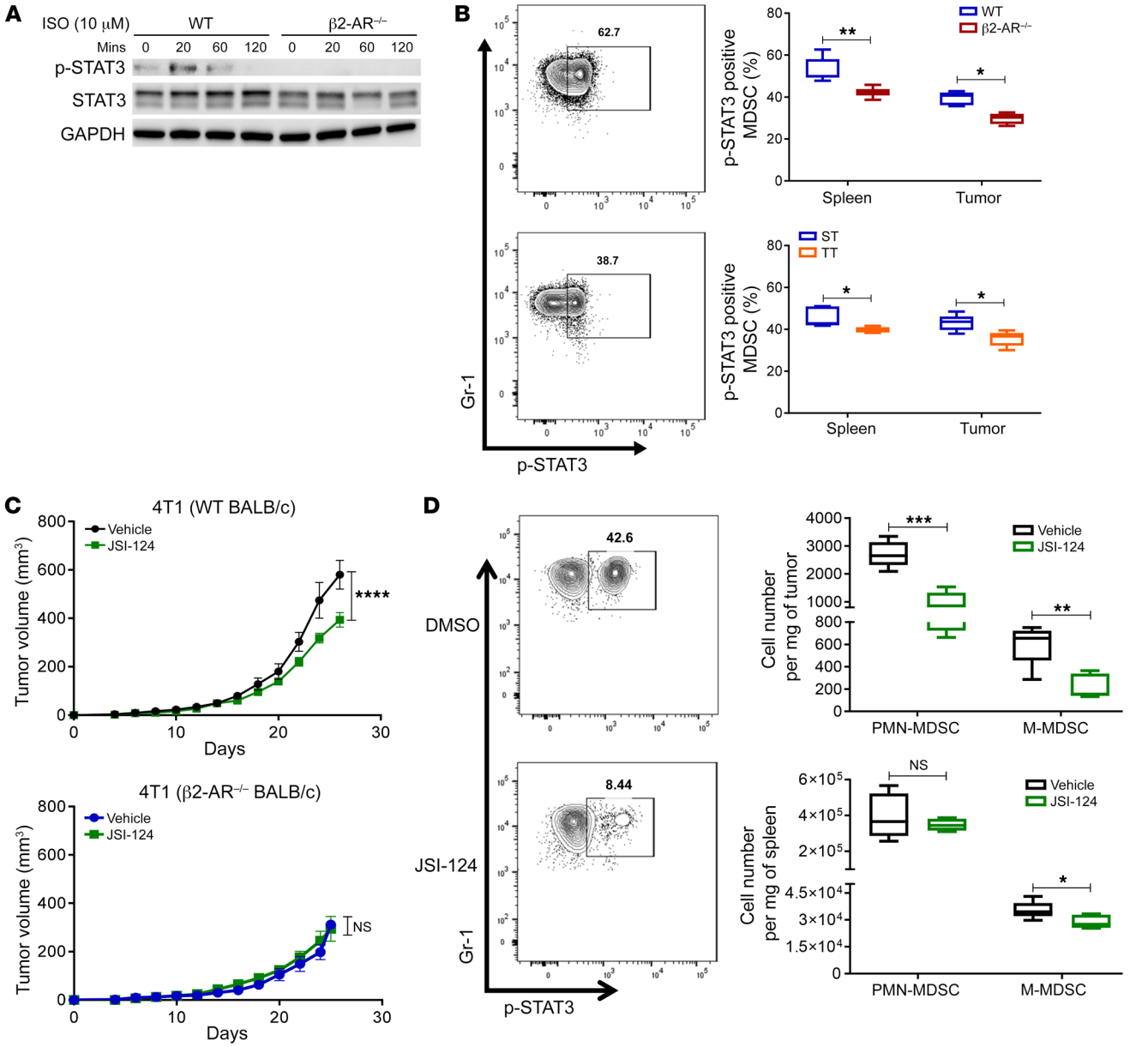

Figure 5. β2-AR stimulation in MDSCs activates STAT3 signaling. (**A**) Bone marrow MDSCs sorted from 4T1 tumor–bearing mice were treated with or without ISO and the level p-STAT3 was analyzed by Western blot (representative blot shown). (**B**) p-STAT3 expression in tumor MDSCs in WT or β2-AR$^{-/-}$ tumor–bearing mice (top) or WT tumor bearing mice housed at ST or TT (bottom), using flow cytometry (n = 10, 2 replicates). (**C**) Tumor growth kinetics in WT or β2-AR$^{-/-}$ 4T1 tumor–bearing mice receiving DMSO or JSI-124 (1 mg/kg, i.p., daily injection) (n = 6–10 mice from 2 replicates). (**D**) MDSC absolute number in spleen or tumor of WT 4T1 tumor–bearing mice receiving DMSO or JSI-124 (n = 5). Two-way ANOVA was used to analyze statistical significance among tumor growth in different groups. These data are presented as mean ± SEM. Other data are presented as median ± minimum to maximum, and the Student's t test was used to analyze statistical significance between 2 groups. In all panels, $^{*}P < 0.05$, $^{**}P < 0.01$, $^{***}P < 0.001$, and $^{****}P < 0.0001$. A P value less than 0.05 was considered significant.

lol (a pan β-AR blocker) in our murine tumor models. As we previously reported (28), propranolol significantly slows tumor growth in WT mice but not β2-AR$^{-/-}$ mice (Figure 6A). In addition, the numbers of MDSCs in tumor tissue and spleen of WT mice were decreased compared with WT mice receiving the vehicle control (Figure 6B). We then performed immunohistochemistry (IHC) on tumor tissue, and found a decreased number of myeloid cells and a decreased expression of angiogenic markers (CD31 and VEGF-α) in the tumors of mice treated with propranolol compared with tumors of mice from the control group (Figure 6C). Next, we tested the effects of the β2-AR–specific agonist (salbutamol) on tumor growth and MDSC accumulation. We found that salbutamol increased both tumor growth (Supplemental Figure 5A) and MDSC accumulation in the spleen (Supplemental Figure 5B) and tumor tissue (Supplemental Figure 5C) in mice housed under ST conditions. To rule out the possibility of indirect effects of propranolol on tumor growth and MDSC accumulation, we used 6-hydroxydopamine (6-OHDA) to deplete nerve-derived NE. We found that treatment of WT mice housed at ST with 6-OHDA significantly decreased MDSC accumulation in both the spleen and

tumor tissue, but it was less efficient than propranolol, suggesting that nerves are not the only source of NE (Figure 6, D and E). These results demonstrate that the protumor effects of chronic stress mediated by β2-AR signaling in MDSCs can be regulated by commonly used β-blocker drugs.

β2-AR activation increases MDSC generation from human PBMCs. We tested whether the presence of neurotransmitters released into the vasculature (which would happen under physiological conditions) could influence the generation of MDSCs in human blood. We isolated human peripheral blood mononuclear cells (PBMCs) from healthy volunteers, and cultured them to generate MDSCs in the presence or absence of ISO as described (37). We found that PBMC-derived MDSCs express β2-AR on their surface (Figure 7A) and that addition of ISO, which provides stimulation of these receptors, significantly increased the generation of MDSCs ($CD14^+CD33^+$) 7 days after culture (Figure 7B). We also found that adding ISO into MDSC culture media increased the expression of arginase-I, PD-L1, and p-STAT3, thus replicating in human cells the effects that β2-AR activation has in mouse MDSCs (Figure 7C). Then, to investigate the immunosuppressive potency of human cells derived in culture with or without ISO treatment, we isolated these MDSCs from culture and cocultured them with human $CD3^+$ T cells stimulated with anti-CD3 and anti-CD28 beads. ISO-treated cells suppressed proliferation and IFN-γ production of both $CD4^+$ and $CD8^+$ T cells at a higher level compared with that seen using cells cultured without ISO (Figure 7D). These data highlight the potential for increased chronic stress and production of catecholamines in humans to enhance the generation and immunosuppressive function of MDSCs.

Discussion

The immune response can potentially control tumor growth, but its development requires a critical balance between the functions of immune suppressive cells such as MDSCs and immune effector cells such as $CD8^+$ T cells. Previous studies, including those from our lab, have shown that stress (including physical or psychological stress) promotes tumor growth and metastasis and suppresses $CD8^+$ T cell–dependent antitumor immunity (29, 38–40). The data presented here reveal that adrenergic stress signaling also increases the frequency and suppressive function of MDSCs in the tumor microenvironment (TME), spleen, and blood. Using a physiological model of chronic stress (i.e., housing mice in a mild but chronically cool housing temperature), a genetic model (i.e., deletion of β2-AR), and multiple pharmacological interventions, we identified a major role for β2-AR signaling in promoting MDSC survival and protumorigenic function. Overall, the fact that β-AR signaling increases the immune suppressive functions of murine MDSCs in the TME as well as those of human MDSC-like cells generated from PBMCs, points to a mechanism by which chronic stress could tilt the immunological balance toward suppression of the antitumor immune response. Additionally, we found that β2-AR signaling in vivo drives MDSC survival through STAT3 activation. These findings that chronic adrenergic stress promotes the immunosuppressive functions of MDSCs to constrain the antitumor immune response are clinically relevant since cancer patients often report increased symptoms of chronic stress (anxiety, pain, or depression), which are also mediated through the sympathetic nervous system and adrenergic signaling (14, 41).

Mechanistically, physiological and/or psychological stressors provide the stimulus that drives activation of the SNS, leading to increased release of NE from sympathetic nerve endings found systemically and, in particular, in the TME (42). Our work suggests that this elevated adrenergic tone is responsible for observed changes in immune cell populations, and overall promotes a protumor milieu in the TME. Recent data reported by others show that tumors recruit and are innervated by SNS fibers (13, 43), thus providing a conduit for chronic stress to provide signals to the tumor microenvironment. Our data reveal that MDSCs are highly sensitive to these signals and could mediate tumor progression in response to even mild, but chronic, stress such as the thermal stress model used in this study. It is noteworthy that some of our data, while statistically significant, show a relatively modest impact of adrenergic receptor signaling (e.g., Supplemental Figure 1, A–C). It is important to remember that chronic stress is a physiological perturbation and therefore not likely to result in major immunological changes. Nevertheless, a daily suboptimal immune control of tumor progression, over long periods of time, could result in a significant increase in tumor progression and/or metastases. This point is reinforced by recent epidemiological data coming from several different cancer settings, supporting the idea that daily use of β-blockers, for indications unrelated to cancer, is associated with improved response to therapy and increased overall survival (44).

A positive correlation between chronic stress and increased numbers of MDSCs has been shown in several settings other than cancer. A recent report by McKim et al. (45) has shown that psychological stress (exposure to an aggressor mouse) increases hematopoietic stem progenitor cell (HSPC) trafficking from bone marrow to spleen, and promotes differentiation into several types of immunosuppressive cells, including MDSCs. Another report has shown that NE increases proliferation of granulocyte-monocyte progenitors (GMPs) in the spleen and that severing splenic SNS nerves diminishes GMP proliferation and MDSC development (18).

In further support of our findings, Ben-Shaanan et al. showed that positive emotions decrease NE levels in the bone marrow, diminish the generation of MDSCs, and reduce the inhibitory effects of MDSCs on T cell proliferation and effector phenotype in mouse tumor models (46). These data support our results indicating that decreasing NE-mediated β2-AR signaling in MDSCs reduces the capacity of MDSCs to suppress T cell proliferation along with reducing expression of components of major inhibitory pathways.

We also found that a higher percentage of MDSCs in the spleens of tumor-bearing mice express β2-AR compared with those of tumor-free mice, and that soluble factors (e.g., inflammatory cytokines including GM-CSF) derived from tumor cells, stromal cells, or immune cells promote β2-AR upregulation. In agreement with our results, a recent report confirmed that the expression level of β2-AR on MDSCs residing in various tissues is different (46), suggesting that the effects of chronic stress on MDSCs in those tissues could be regulated by this differential expression level of β2-AR.

The pivotal role of STAT3 in MDSC expansion and MDSC-mediated immunosuppression has been widely reported (35). STAT3 activity is also the predominant signaling molecule in TAMs

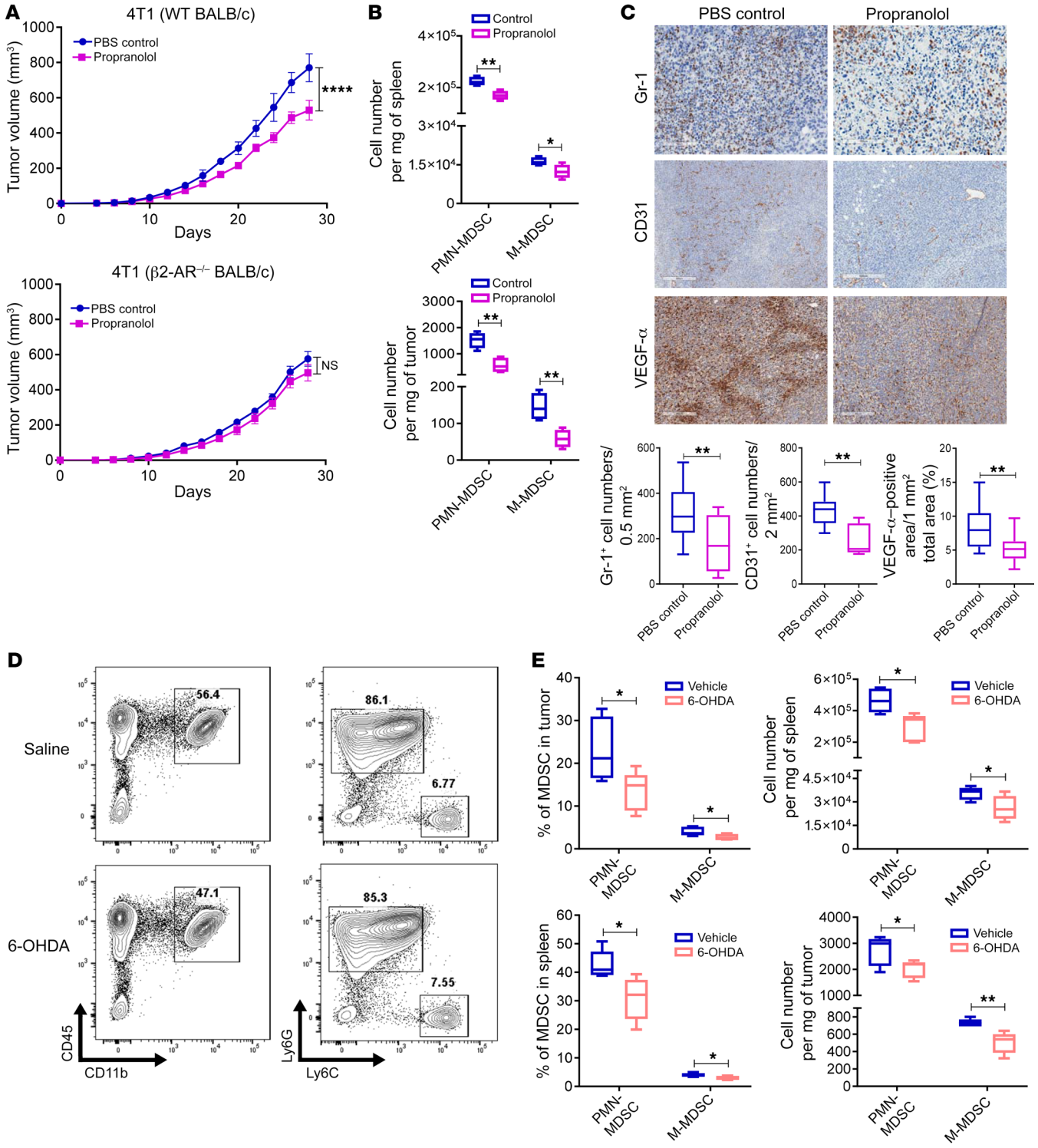

Figure 6. Propranolol suppresses tumor growth and decreases MDSC accumulation in the spleen and tumor tissue. (**A**) Tumor growth kinetics in WT or β2-AR$^{-/-}$ mice orthotopically injected with 4T1 tumor cells receiving PBS or propranolol (i.p. daily injection) (n = 10). (**B**) Absolute number of MDSCs in spleen and tumor of WT mice treated with PBS or propranolol. (**C**) Tumor tissue was collected in WT 4T1 tumor–bearing mice at day 25 and stained for Gr-1 (×20 magnification), CD31 (×4 magnification), and VEGF-α (×10 magnification) (n = 5). (**D**) Representative flow cytometry plot of MDSCs in WT or β2-AR$^{-/-}$ 4T1 tumor–bearing mice receiving saline or 6-OHDA (50 mg/kg, i.p., weekly injection) (n = 6–10 mice from 2 replicates). (**E**) Percentage and absolute number of MDSCs in tumor and spleen of 4T1 tumor–bearing mice receiving saline or 6-OHDA (50 mg/kg, i.p., weekly injection) (n = 5). Two-way ANOVA was used to analyze statistical significance among tumor growth in different groups. These data are presented as mean ± SEM. Other data are presented as median ± minimum to maximum, and the Student's t test was used to analyze statistical significance between 2 groups. In all panels, $^{*}P < 0.05$, $^{**}P < 0.01$, and $^{****}P < 0.0001$. A P value less than 0.05 was considered significant.

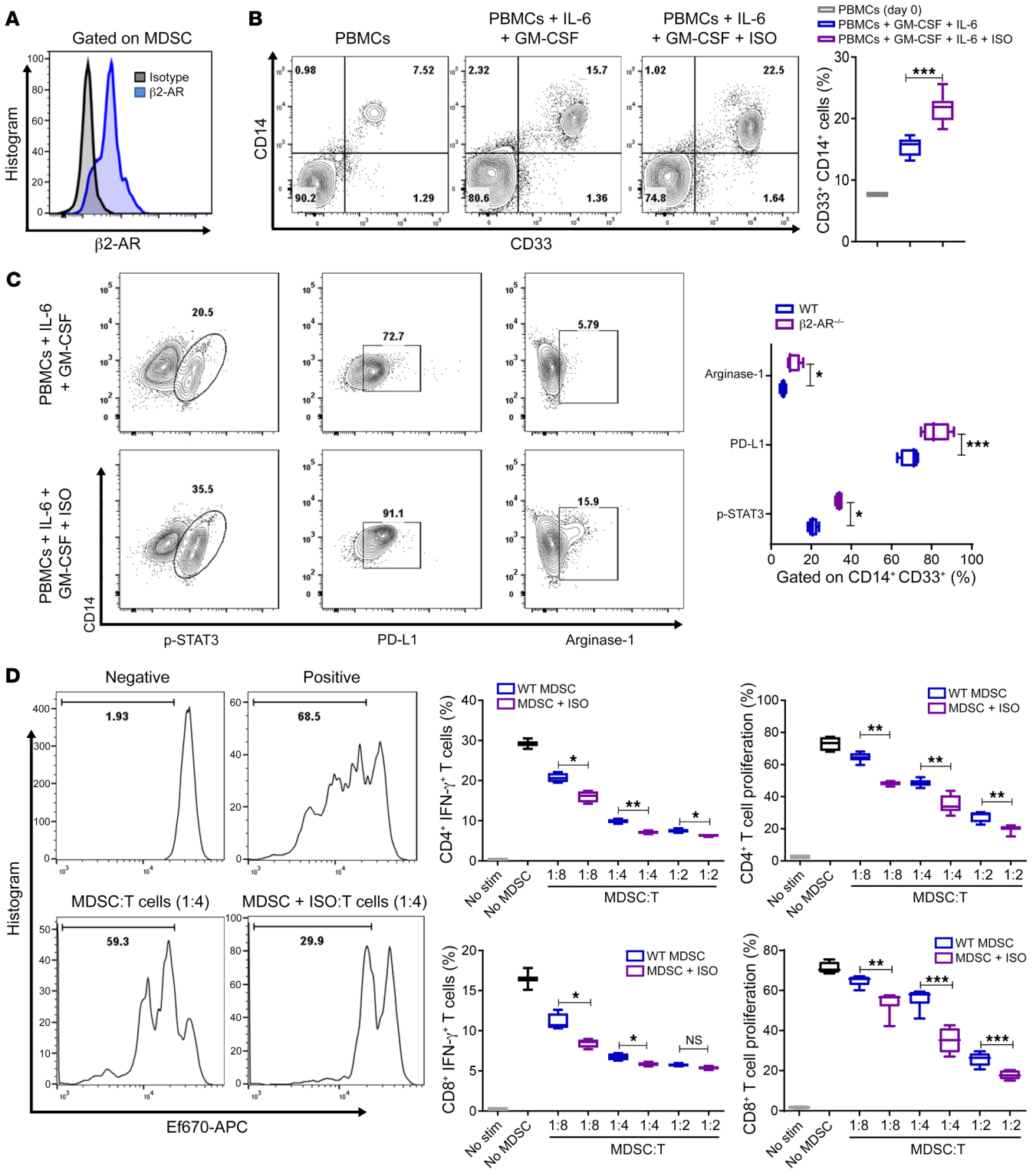

Figure 7. Isoproterenol increases MDSC generation from human PBMCs. (**A**) Analysis of β2-AR expression on MDSC surface analyzed by flow cytometry after culturing PBMCs with IL-6 and GM-CSF with or without ISO for 7 days. (**B**) Analysis of MDSC generation analyzed by flow cytometry after culturing PBMCs with IL-6 and GM-CSF with or without ISO for 7 days. (**C**) The expression of p-STAT3, PDL-1, and arginase-I after culturing PBMCs with IL-6 and GM-CSF with or without ISO for 7 days. (**D**) Effects of in vitro differentiated MDSCs in the presence or absence of ISO on allogenic $CD4^+$ or $CD8^+$ T cell proliferation and IFN-γ production. One histogram example corresponding to $CD8^+$ proliferation analyzed by ef670 dilution dye in a ratio of 1:4 is shown. These data are presented as median ± minimum to maximum from 3 biological replicates in all graphs, and the Student's *t* test was used to analyze statistical significance between 2 groups. In all panels, $^*P < 0.05$, $^{**}P < 0.01$, and $^{***}P < 0.001$. A *P* value less than 0.05 was considered significant.

of different cancers, including glioblastoma (47). It has been shown that STAT3 activation plays crucial roles in myelopoiesis, and constitutive phosphorylation of STAT3 in myeloid cells increases the accumulation of MDSCs in spleen and tumor tissues (48). Here, we showed that β2-AR activation in MDSCs activates STAT3 phosphorylation, suggesting that the importance of STAT3 activity in MDSC biology, and possibly TAM biology, is mediated at least in part by β2-AR signaling. This upregulation of STAT3 activity is a likely mechanism underlying the increased MDSC survival and changes in immune-inhibitory function that we observed.

It is well-known that the Fas and FasL interaction plays an important regulatory role in lymphocyte homeostasis (49). Apoptosis mediated by the expression of Fas receptor on MDSCs and FasL on T cells, in particular $CD8^+$ T cells, plays a key role in MDSC survival and turnover (50), and it has been shown that this process is impaired in tumor-bearing mice, resulting in increased MDSC accumulation (34, 50, 51). Immunotherapy using either IL-12/αCD40 (52) or irradiation plus anti–PD-1 activates cytotoxic T cells and promotes MDSC apoptosis (53). In our study, we showed that β2-AR activation in MDSCs increases the resistance of MDSCs to apoptosis induced by Fas/FasL. We found that the expression of the Fas receptor and the level of apoptosis were higher in MDSCs lacking β2-ARs. We also confirmed, by in vivo competition assays, that the level of apoptosis is increased in β2-AR–deficient MDSCs. Although the precise mechanisms by which β2-ARs regulate the expression of Fas require further investigation, these data provide new evidence about the important role of β2-AR in MDSC resistance to apoptosis. In addition, these data provide insight into the potential application of β2-AR blockers in combination with various treatments like immunotherapies (including anti–PD-1) and irradiation to improve the antitumor immune response through increased susceptibility of MDSCs to cell death.

In summary, our work demonstrates that chronic stress, acting through the β2-AR, significantly promotes proliferation, suppressive function, and survival of MDSCs and therefore has the potential to significantly suppress the antitumor immune response. Inhibiting β2-AR signaling by β-AR blockade, inhibiting NE releasing nerves, or β2-AR deletion can decrease the accumulation of MDSCs, reduce their immunosuppressive functions, and is associated with the increased efficacy of the antitumor immune response and inhibition of tumor growth that we have previously seen. Understanding the mechanisms by which the expression of β2-AR can be regulated in immune cells in different organs warrants further investigation. Our data also provide justification for further investigation of the therapeutic potential of blocking chronic stress–mediated β2-AR signaling. Interventions focusing on this strategy have the potential to significantly improve cancer treatment outcomes, with the additional benefit of having minimal toxicity compared with other cancer therapies. Although additional research on drugs that specifically block β2-ARs is needed to increase the precision of this therapy, we have shown that pharmacologic agents like propranolol, which are currently clinically available and FDA-approved, could be a potentially efficacious approach at the present time.

Methods

Animals and tumor cells. BALB/c (H-2^d), C57BL/6 (H-2^b, CD45.1), and C57BL/6 (H-2^b, CD45.2) mice were purchased from Charles River. β2-AR knockout (β2-$AR^{-/-}$) mice on a BALB/c background were of the gift of David Farrar (UT Southwestern Medical Center). β2-AR knockout mice on C57BL/6 were developed at Roswell Park. GFP-positive mice on C57BL/6 background were gifted by Michael Nemeth (Roswell Park). All mice were maintained in SPF housing, all experiments were performed in accordance with the animal care guidelines at Roswell Park Comprehensive Cancer Center, and all protocols used were approved by the animal studies committee. 6-OHDA (162957), propranolol (P0884), salbutamol (S8260), and isoproterenol (16504) were purchased from MilliporeSigma. Cucurbitacin I (JSI-124) was purchased from TOCRIS, R&D Systems.

Cell culture and tumor models. 4T1 tumor cells were purchased from ATCC (ATCC, catalog CRL-2539). AT-3 tumor cells were provided by Scott Abrams (Roswell Park). Cell lines were confirmed to be mycoplasma-negative yearly using the Mycoplasma Plus PCR Primer Set (Agilent Technologies, catalog 302008). 4T1 cell lines were cultured in RPMI 1640 (Corning Cellgro) supplemented with 10% FBS, 1% L-glutamine, and 1% penicillin/streptomycin. AT-3 tumor cells cultured in DMEM (Corning Cellgro) supplemented with 10% FBS, 1% L-glutamine, and 1% penicillin/streptomycin and 7% CO_2. Once thawed, cells were passed twice prior to use. 4T1 cells (1×10^5) in 100 μL PBS and 5×10^5 AT-3 cells in 100 μL PBS were subcutaneously injected into the fourth mammary fat-pad of female BALB/c and C57/BL6 mice, respectively. Tumor growth was monitored in a blinded manner throughout experiments, and perpendicular diameters (width/length) were measured every 2 days. Tumor volume was calculated using the following equation: tumor volume = $((2W \times L)/2)$ mm^3, where W is the small dimension and L is the large dimension.

Ambient temperature manipulation. Mice were housed 5 per cage in Precision Refrigerated Plant-Growth Incubators (ThermoFisher Scientific) and maintained at either standard temperature (~22°C) or thermoneutral temperature (~30°C) as previously described (27, 54). Humidity was controlled using a Top Fin Air Pump AIR 1000 with Top Fin tubing. Mice were acclimated to the assigned temperature for at least 2 weeks prior to tumor injection.

Reagents and antibodies. Antibodies including anti–mouse CD3 (clone 17A2), CD4 (clone GK1.5), CD8 (clone 53-6.7), CD45 (clone 30F11), Gr-1 (clone RB6-8C5), CD45.1 (clone A20), CD45.2 (clone 104), CD11b (clone M1/70), PD-L1 (clone MIH5) CD206 (clone C068C2), F4/80 (clone BM8), Ly6C (clone HK1.4), Ly6G (clone 1A8), Arginase-I (clone IC5868F, R&D Systems), Bcl-2 (clone BCL/10C4), p-STAT3 (clone 13A3-1), Fas (clone 15A7), FasL (clone MFL-3), and Caspase-8 (clone FITC-IETD-FMK) were purchased from Biolegend, BD Bioscience, and eBioscience, except as noted. Antibodies including anti–human CD33 (clone P67.6), CD14 (clone M5E2), CD4 (clone A161A1), CD8 (clone RPA-T6), Arginase-I (clone 14D2C43), p-STAT3 (clone 13A3-1), β2-AR (clone R11E1), and PDL-1 (clone 29E2A3) were purchased from Biolegend. Mouse MDSC isolation kit was purchased from Miltenyi Biotec. EasySep Human T Cell Isolation Kit and EasySep HLA chimerism whole-blood CD33 positive selection kit were obtained from Stem Cell Technologies. Mouse and human IL-6, GM-CSF, and G-CSF were purchased from Biolegend. Apoptosis levels were measured by flow cytometry using an apoptosis kit (ebioscience, ThermoFisher Scientific) based on the manufacturer's protocol.

eFluor 670 dilution. Single-cell suspensions of sorted pan T cells were suspended in 5 mL of 37°C PBS. An equal volume of 10 μM eFluor 670 (ebioscience, ThermoFisher Scientific) in 37°C PBS was added

to the T cell suspension and incubated for 10 minutes at 37°C. After incubation, 5 mL RPMI 1640 containing 10% FBS was added, and cells were washed.

Coculture of MDSCs and T cells. MDSCs were sorted from 4T1 tumor–bearing mice or PBMC-derived MDSCs using mouse or human MDSC isolation kit (Stem Cell Technologies). $CD4^+$ and $CD8^+$ cells were harvested from BALB/c mice or human PBMCs by using Pan T Cell Isolation Kit II (Miltenyi Biotec) and EasySep Human T Cell Isolation Kit (Stem Cells Technologies) respectively. MDSCs were cocultured with 2×10^5 $CD3^+$ T cells in RPMI 1640 culture media supplemented with L-glutamine, penicillin/streptomycin, and 10% heat-inactivated FBS. After 72 hours, cells were collected and eFluor 670 dilutions were calculated by gating from live $CD4^+$ or $CD8^+$ T cells using flow cytometry. To activate mouse T cells, CD3 and CD28 antibodies (both from BioXCell) were added to a coculture of T cells and MDSCs. To stimulate human T cells, CD3 and CD28 beads (Invitrogen) were used. Cytokine production by T cells in coculture was detected by adding Brefeldin A (Invitrogen) 4 hours before staining.

Luminex assay. Plasma was collected by retro-orbital bleeding on the indicated days following transplant. Blood samples were placed on ice until all samples had been collected. Once the final sample was collected, all samples were incubated at room temperature for 20 minutes to allow for coagulation to occur. After incubation, vials were centrifuged at 4°C for 10 minutes at 2000 *g*. Serum plasma was collected and frozen at –80°C. Mouse cytokine and chemokine 11–plex was performed by Flow and Image Cytometry, Luminex Division at Roswell Park, as per the manufacturer's instructions.

Histopathology scoring. WT and β2-$AR^{-/-}$ mice were injected with 1×10^5 4T1 cells in 100 μL PBS; mice were sacrificed 25 days after injection. Lungs were removed, fixed with formalin, sectioned, and stained with H&E.

Bone marrow chimeras. Chimeras were generated between BALB/c WT and β2-$AR^{-/-}$ hosts. These mice were lethally irradiated with 8.5 Gy of total body irradiation (Cesium 137 source). One day after irradiation, BM was reconstituted with the intravenous (tail vein) injection of 5×10^6 BM cells and 5×10^6 splenocytes which were isolated from healthy β2-$AR^{-/-}$ mice or WT controls. After 8 weeks, tumor growth experiments were conducted and mice were injected with 1×10^5 4T1 cells in 100 μL PBS.

Propranolol (β-blocker), salbutamol (β2-agonist), and isoproterenol (β-agonist) studies. For studies in which propranolol was used to assess the impact of adrenergic signaling on tumor growth and MDSC accumulation, tumor-bearing mice were housed at ST (22°C) or TT (~30°C). Propranolol treatment was initiated 4 days prior to tumor cell implantation and daily treatment continued until the experimental endpoint. Mice received 200 μg propranolol (clone P0884, Sigma-Aldrich) in 10 mg/kg by i.p. injection; control mice received 200 μL PBS. Salbutamol (clone S8260, Sigma-Aldrich) was injected 1 mg/kg daily after tumor implantation. For in vitro studies, ISO (clone 16504, Sigma-Aldrich) was used at 10 μM and 100 μM concentrations and propranolol (clone P0884, Sigma-Aldrich) was used at 10 μM.

MDSC depletion. Anti–mouse Gr-1 antibody (clone RB6-8C5) and IgG2a isotype control antibody (clone LTF-2) were purchased from BioXCell. WT and β2-$AR^{-/-}$ mice were randomized to receive treatment with either anti–Gr-1 antibody (200 μg) or an isotype antibody (200 μg). Treatment was initiated on a rolling basis beginning one day after tumors became detectable. Mice received 5 injections of antibody spaced 4 days apart.

Flow cytometry. Single-cell suspensions were created by excising and cutting mouse tumors into 2- to 3-mm pieces. 4T1 tumors were dissociated with collagenase/hyaluronidase (clone 07912, Stem Cell Technologies) following the manufacturer's protocol prior to passage through a 70 μm nylon cell strainer (Corning). Spleens were mechanically disrupted and directly passed through a 70-μm nylon cell strainer (Corning). Red blood cells were lysed using ACK buffer (Gibco). Cells were then washed with flow running buffer (0.1% BSA in PBS) and incubated with anti-CD16/32 (Fc receptors blocker, 1:200) at 4°C for 10 minutes. Cells were then stained with the different antibodies. Live/dead aqua or yellow dye (ThermoFisher Scientific) were used to gate out dead cells. For intracellular staining, cells were first surface-stained as above, fixed and permeabilized using the FoxP3/Transcription Factor Staining Buffer Set (eBiosciences) as per the manufacturer's protocol, then stained with antibodies to intracellular antigens. All data were collected on a LSR Fortessa flow cytometer (BD Biosciences) and analyzed with FlowJo v7 software (Tree Star, Inc.). Absolute number of cells in both spleen and tumor tissues was calculated by multiplying percentage of live $CD45^+$ $CD11b^+$ $Ly6G^+$ (PMN-MDSC) and live $CD45^+$ $CD11b^+$ $Ly6C^+$ (M-MDSC) by the cell numbers of the sample, divided by milligram weight.

Cell sorting. MDSCs were harvested from WT and β2-$AR^{-/-}$ 4T1 tumor–bearing mice for Nanostring analysis. MDSCs were sorted from single-cell suspensions of tumors excised 25 days after 4T1 tumor implantation into WT and β2-$AR^{-/-}$ mice. Cell sorting was performed using a BD FACSAria (BD Biosciences).

Western blot. MDSCs were sorted from bone marrow of 4T1 tumor–bearing WT and β2-$AR^{-/-}$ mice using a murine MDSC isolation kit. MDSCs were suspended in 4 mL RPMI 1640 culture media supplemented with L-glutamine, penicillin/streptomycin, and 10% heat inactivated FBS in 2 cm^2, 24-well plates (Costar, catalog 3524). Cells were incubated at 37°C and treated with 100 μM ISO in PBS for 20, 60, or 120 minutes. Control cells were treated with PBS. After treatment time, cells were washed with PBS and frozen at –80°C. A lysis buffer consisting of RIPA Buffer (Pierce, catalog 89900), protease and phosphatase inhibitor mini tablets (Pierce, catalog A32961), and 0.1M PMSF (ThermoFisher Scientific, catalog 36978) was used to extract protein from MDSC samples. BCA assays were carried out using a clear, flat-bottom, 96-well plate (Costar, catalog 9018), the BCA Protein Assay Kit (Pierce, catalog 23225), and a plate reader (Synergy H1) to determine the concentration of protein in each sample. Protein resolution was achieved by SDS-PAGE, transferred to a polyvinylidene difluoride membrane (Millipore, catalog IPVH00010), and blocked with 5% nonfat milk or 5% BSA (ThermoFisher Scientific, catalog 10857) in Tris buffered saline (Bio-Rad, catalog 173-6435) with Tween 20 (Bio-Rad, catalog 170-6531) per primary antibody incubation specifications. Membranes were probed overnight at a concentration of 1:1000 for phospho-STAT3 (Cell Signaling, catalog 9145), STAT3 (Cell Signaling, catalog 9139), and GAPDH (Cell Signaling, catalog 5174). Anti-rabbit (Cell Signaling, catalog 7074) and anti-mouse (Cell Signaling, catalog 7076) horseradish peroxidase–conjugate secondary antibodies were used at a concentration of 1:3000. Membranes were developed with ECL-substrate (Bio-Rad, catalog 170-5060) and images were captured using the LI-COR Odyssey Fc (catalog OFC-0756).

Generation of human MDSCs from PBMCs. Human PBMCs were isolated from healthy volunteer donors by venipuncture and subsequent

differential density gradient separation (Ficoll Hypaque, MilliporeSigma). PBMCs were cultured in T-25 flasks at 1×10^6 cells/mL in complete medium (RPMI 1640, Corning Cellgro) supplemented with the cytokines IL-6 (20 ng/mL, MilliporeSigma) and GM-CSF (20 ng/mL, R&D Systems) for 7 days, in the presence or absence of ISO (10 μM). Cultures were run in duplicate, and medium and cytokines were refreshed every 2–3 days. After 1 week, all cells were collected from PBMC cultures. Adherent cells were removed using non–protease cell detachment solution Detaching (Genlantis). At day 7, MDSC populations were characterized using CD14 and CD33 markers by flow cytometry. $CD33^+$ cells were isolated from each culture using EasySep HLA Chimerism CD33 Whole Blood Positive Selection Kit (STEMCELL Technologies) per manufacturer's instructions. The purity of isolated cell populations was determined to be greater than 90% by flow cytometry.

Nanostring. Sorted MDSCs ($CD11b^+$ $Gr\text{-}1^+$) from WT or $\beta2\text{-}AR^{-/-}$ mice bearing 4T1 tumors were prepared for Nanostring analysis. In brief, RNA was isolated from sorted cells using the RNeasy Plus Mini kit (Qiagen). Nanostring analysis was performed with the nCounter Analysis System at NanoString Technologies. The nCounter Mouse Immunology Kit, which includes 561 immunology-related mouse genes, was used.

Statistics. The Student's *t* test was used to compare data between 2 groups, 2-way ANOVA with Tukey's post hoc analysis was used to generate tumor growth statistics using GraphPad Prism, and 1-way ANOVA with Tukey's post hoc analysis was used to compare data between 3 groups or more using GraphPad Prism. All tumor growth data are presented as mean ± SEM, and all other data are presented as median ± minimum to maximum.

Study approval. The Roswell Park Comprehensive Cancer Center IRB approved human subject studies (NHR 009510). Generation of the mice and all mice studies were reviewed and approved by the Roswell Park Comprehensive Cancer Center IACUC (protocol numbers 757M and 1038M).

Author contributions

HM initiated the study. HM, BLH, SIA, and EAR designed the study; HM performed the experiments with assistance from CRM, GQ, BD, and MC. HM, BLH, PLM, SIA, and EAR analyzed and interpreted the data and wrote the paper.

Acknowledgments

The authors thank Jeanne M. Prendergast, Samuel A. Ministero, Sean H. Colligan, Heather M. Campbell, and Benjamin L.S. McCarthy for technical assistance, Michael J. Nemeth (Roswell Park Comprehensive Cancer Center (Roswell Park) and David Farrar (University of Texas Southwestern Medical Center) for the generous gifts of GFP^+ mice and $\beta2AR^{-/-}$ mice (in BALB/c background), respectively, and the Genomics Shared Resource (Roswell Park) and the Roswell Park Flow Cytometry Core Facility for expert support. This project was supported by National Institutes of Health grants R01 CA205246 and R01 CA099326 (to EAR), the Roswell Park Alliance Foundation, Breast Cancer Coalition of Rochester, and NCI grant P30CA016056. SIA was supported by NIH grant R01 CA172105.

Address correspondence to: Elizabeth A. Repasky, Department of Immunology, Roswell Park Comprehensive Cancer Center, Elm and Carlton Streets, Buffalo, New York, 14263, USA. Phone: 716.845.3133; Email: elizabeth.repasky@roswellpark.org.

1. Ugel S, De Sanctis F, Mandruzzato S, Bronte V. Tumor-induced myeloid deviation: when myeloid-derived suppressor cells meet tumor-associated macrophages. *J Clin Invest*. 2015;125(9):3365–3376.
2. Veglia F, Perego M, Gabrilovich D. Myeloid-derived suppressor cells coming of age. *Nat Immunol*. 2018;19(2):108–119.
3. Netherby CS, Abrams SI. Mechanisms overseeing myeloid-derived suppressor cell production in neoplastic disease. *Cancer Immunol Immunother*. 2017;66(8):989–996.
4. Ostrand-Rosenberg S. Myeloid derived-suppressor cells: their role in cancer and obesity. *Curr Opin Immunol*. 2018;51:68–75.
5. Condamine T, Ramachandran I, Youn JI, Gabrilovich DI. Regulation of tumor metastasis by myeloid-derived suppressor cells. *Annu Rev Med*. 2015;66:97–110.
6. Bronte V, et al. Recommendations for myeloid-derived suppressor cell nomenclature and characterization standards. *Nat Commun*. 2016;7:12150.
7. Gabrilovich DI. Myeloid-derived suppressor cells. *Cancer Immunol Res*. 2017;5(1):3–8.
8. Waight JD, et al. Myeloid-derived suppressor cell development is regulated by a STAT/IRF-8 axis. *J Clin Invest*. 2013;123(10):4464–4478.
9. Ostrand-Rosenberg S, Fenselau C. Myeloid-derived suppressor cells: immune-suppressive cells that impair antitumor immunity and are sculpted by their environment. *J Immunol*. 2018;200(2):422–431.
10. Eng JW, Kokolus KM, Reed CB, Hylander BL, Ma WW, Repasky EA. A nervous tumor microenvironment: the impact of adrenergic stress on cancer cells, immunosuppression, and immunotherapeutic response. *Cancer Immunol Immunother*. 2014;63(11):1115–1128.
11. Qiao G, Chen M, Bucsek MJ, Repasky EA, Hylander BL. Adrenergic signaling: a targetable checkpoint limiting development of the antitumor immune response. *Front Immunol*. 2018;9:164.
12. Eng JW, et al. Housing temperature-induced stress drives therapeutic resistance in murine tumour models through β2-adrenergic receptor activation. *Nat Commun*. 2015;6:6426.
13. Magnon C, et al. Autonomic nerve development contributes to prostate cancer progression. *Science*. 2013;341(6142):1236361.
14. Cole SW, Nagaraja AS, Lutgendorf SK, Green PA, Sood AK. Sympathetic nervous system regulation of the tumour microenvironment. *Nat Rev Cancer*. 2015;15(9):563–572.
15. Sloan EK, et al. The sympathetic nervous system induces a metastatic switch in primary breast cancer. *Cancer Res*. 2010;70(18):7042–7052.
16. Jobling P, Pundavela J, Oliveira SM, Roselli S, Walker MM, Hondermarck H. Nerve-cancer cell cross-talk: a novel promoter of tumor progression. *Cancer Res*. 2015;75(9):1777–1781.
17. Armaiz-Pena GN, Cole SW, Lutgendorf SK, Sood AK. Neuroendocrine influences on cancer progression. *Brain Behav Immun*. 2013;30(Suppl):S19–S25.
18. Vasamsetti SB, et al. Sympathetic neuronal activation triggers myeloid progenitor proliferation and differentiation. *Immunity*. 2018;49(1):93–106.e7.
19. Katritch V, Cherezov V, Stevens RC. Structure-function of the G protein-coupled receptor superfamily. *Annu Rev Pharmacol Toxicol*. 2013;53:531–556.
20. Lorton D, Bellinger DL. Molecular mechanisms underlying β-adrenergic receptor-mediated cross-talk between sympathetic neurons and immune cells. *Int J Mol Sci*. 2015;16(3):5635–5665.
21. Sanders VM. The beta2-adrenergic receptor on T and B lymphocytes: do we understand it yet? *Brain Behav Immun*. 2012;26(2):195–200.
22. McAlees JW, Smith LT, Erbe RS, Jarjoura D, Ponzio NM, Sanders VM. Epigenetic regulation of beta2-adrenergic receptor expression in T(H)1 and T(H)2 cells. *Brain Behav Immun*. 2011;25(3):408–415.
23. Estrada LD, Ağaç D, Farrar JD. Sympathetic neural signaling via the β2-adrenergic receptor suppresses T-cell receptor-mediated human and mouse CD8(+) T-cell effector function. *Eur J Immunol*. 2016;46(8):1948–1958.
24. Mohammadpour H, O'Neil R, Qiu J, McCarthy PL, Repasky EA, Cao X. Blockade of host β2-adrenergic receptor enhances graft-versus-tumor

effect through modulating APCs. *J Immunol*. 2018;200(7):2479–2488.
25. Kokolus KM, Spangler HM, Povinelli BJ, Farren MR, Lee KP, Repasky EA. Stressful presentations: mild cold stress in laboratory mice influences phenotype of dendritic cells in naive and tumor-bearing mice. *Front Immunol*. 2014;5:23.
26. Schmidt D, Peterlik D, Reber SO, Lechner A, Männel DN. Induction of suppressor cells and increased tumor growth following chronic psychosocial stress in male mice. *PLoS ONE*. 2016;11(7):e0159059.
27. Kokolus KM, et al. Baseline tumor growth and immune control in laboratory mice are significantly influenced by subthermoneutral housing temperature. *Proc Natl Acad Sci USA*. 2013;110(50):20176–20181.
28. Bucsek MJ, et al. β-Adrenergic signaling in mice housed at standard temperatures suppresses an effector phenotype in $CD8^+$ T cells and undermines checkpoint inhibitor therapy. *Cancer Res*. 2017;77(20):5639–5651.
29. Hylander BL, Gordon CJ, Repasky EA. Manipulation of ambient housing temperature to study the impact of chronic stress on immunity and cancer in mice. *J Immunol*. 2019;202(3):631–636.
30. Gordon C. Thermal physiology of laboratory mice: defining thermoneutrality. *J Therm Biol*. 2012;37(8):654–685.
31. Fan X, Wang Y. β2 Adrenergic receptor on T lymphocytes and its clinical implications. *Pro Nat Sci*. 2009;19(1):17–23.
32. Morales JK, Kmieciak M, Knutson KL, Bear HD, Manjili MH. GM-CSF is one of the main breast tumor-derived soluble factors involved in the differentiation of CD11b-Gr1- bone marrow progenitor cells into myeloid-derived suppressor cells. *Breast Cancer Res Treat*. 2010;123(1):39–49.
33. He YM, et al. Transitory presence of myeloid-derived suppressor cells in neonates is critical for control of inflammation. *Nat Med*. 2018;24(2):224–231.
34. Peyvandi S, et al. Fas ligand deficiency impairs tumor immunity by promoting an accumulation of monocytic myeloid-derived suppressor cells. *Cancer Res*. 2015;75(20):4292–4301.
35. Su YL, Banerjee S, White SV, Kortylewski M. STAT3 in tumor-associated myeloid cells: multitasking to disrupt immunity. *Int J Mol Sci*. 2018;19(6):E1803.
36. Blaskovich MA, Sun J, Cantor A, Turkson J, Jove R, Sebti SM. Discovery of JSI-124 (cucurbitacin I), a selective Janus kinase/signal transducer and activator of transcription 3 signaling pathway inhibitor with potent antitumor activity against human and murine cancer cells in mice. *Cancer Res*. 2003;63(6):1270–1279.
37. Lechner MG, Liebertz DJ, Epstein AL. Characterization of cytokine-induced myeloid-derived suppressor cells from normal human peripheral blood mononuclear cells. *J Immunol*. 2010;185(4):2273–2284.
38. Cole SW, Sood AK. Molecular pathways: beta-adrenergic signaling in cancer. *Clin Cancer Res*. 2012;18(5):1201–1206.
39. Kuol N, Stojanovska L, Apostolopoulos V, Nurgali K. Role of the nervous system in cancer metastasis. *J Exp Clin Cancer Res*. 2018;37(1):5.
40. Hanoun M, Maryanovich M, Arnal-Estapé A, Frenette PS. Neural regulation of hematopoiesis, inflammation, and cancer. *Neuron*. 2015;86(2):360–373.
41. Moreno-Smith M, Lutgendorf SK, Sood AK. Impact of stress on cancer metastasis. *Future Oncol*. 2010;6(12):1863–1881.
42. Faulkner S, Jobling P, March B, Jiang CC, Hondermarck H. Tumor neurobiology and the war of nerves in cancer. *Cancer Discov*. 2019;9(6):702–710.
43. Kamiya A, Hayama Y, Kato S, Shimomura A, Shimomura T, Irie K, et al. Genetic manipulation of autonomic nerve fiber innervation and activity and its effect on breast cancer progression. *Nat neurosci*. 2019;22(8):1289–1305.
44. Kokolus KM, et al. Beta blocker use correlates with better overall survival in metastatic melanoma patients and improves the efficacy of immunotherapies in mice. *Oncoimmunology*. 2018;7(3):e1405205.
45. McKim DB, Yin W, Wang Y, Cole SW, Godbout JP, Sheridan JF. Social stress mobilizes hematopoietic stem cells to establish persistent splenic myelopoiesis. *Cell Rep*. 2018;25(9):2552–2562.e3.
46. Ben-Shaanan TL, et al. Modulation of anti-tumor immunity by the brain's reward system. *Nat Commun*. 2018;9(1):2723.
47. Komohara Y, Ohnishi K, Kuratsu J, Takeya M. Possible involvement of the M2 anti-inflammatory macrophage phenotype in growth of human gliomas. *J Pathol*. 2008;216(1):15–24.
48. Kumar V, et al. CD45 phosphatase inhibits STAT3 transcription factor activity in myeloid cells and promotes tumor-associated macrophage differentiation. *Immunity*. 2016;44(2):303–315.
49. Xu G, Shi Y. Apoptosis signaling pathways and lymphocyte homeostasis. *Cell Res*. 2007;17(9):759–771.
50. Sinha P, Chornoguz O, Clements VK, Artemenko KA, Zubarev RA, Ostrand-Rosenberg S. Myeloid-derived suppressor cells express the death receptor Fas and apoptose in response to T cell-expressed FasL. *Blood*. 2011;117(20):5381–5390.
51. Hu X, et al. Deregulation of apoptotic factors Bcl-xL and Bax confers apoptotic resistance to myeloid-derived suppressor cells and contributes to their persistence in cancer. *J Biol Chem*. 2013;288(26):19103–19115.
52. Weiss JM, et al. Regulatory T cells and myeloid-derived suppressor cells in the tumor microenvironment undergo Fas-dependent cell death during IL-2/αCD40 therapy. *J Immunol*. 2014;192(12):5821–5829.
53. Deng L, et al. Irradiation and anti-PD-L1 treatment synergistically promote antitumor immunity in mice. *J Clin Invest*. 2014;124(2):687–695.
54. Leigh ND, et al. Housing temperature-induced stress is suppressing murine graft-versus-host disease through β2-adrenergic receptor signaling. *J Immunol*. 2015;195(10):5045–5054.